Synthesis and Photophysical Properties of Ferrocene Containing Monomer and Polymer

Vytautas Getautis[1,*]**, Maryte Daskeviciene**[1]**, Tadas Malinauskas**[1]**,** and **Vygintas Jankauskas**[2]

[1] Faculty of Chemical Technology, Kaunas University of Technology, Kaunas, Lithuania
[2] Department of Solid State Electronics, Vilnius University, Vilnius, Lithuania

Summary. Synthesis of a new monomer and polymer containing both ferrocene and hydrazone moieties are reported. The obtained materials were examined by various techniques including differential scanning calorimetry, UV, IR, NMR spectroscopy, and time of flight method. These materials may be of particular interest for the development of future electrophotographic photoreceptors as electron photoemission spectra of the layers showed ionization potentials of 5.35–5.41 eV. The hole drift mobility values in compositions of the designed structures with bisphenol Z polycarbonate exceeded 10^{-8} cm^2/Vs at strong electric fields.

Keywords. Ferrocene; Hydrazones; Epoxides; Polyaddition; Electrophotography.

Introduction

Over the last several years, there has been considerable interest and, consequently, intensive research efforts devoted to design and develop new highly efficient molecular compounds for optoelectronic applications. Ferrocene is a very versatile molecule with important properties, such as high electron density, aromaticity, thermal stability, and redox reversibility. These characteristics together with the ease of preparation of mono-substituted ferrocene derivatives with a great variety of organic and inorganic fragments make it a versatile building block in many fields of research. Ferrocene has mainly attracted the interest of a number of scientists and research groups worldwide because of its applications in material science [1, 2]. Ferrocene derivatives are important in areas requiring special properties, such as electrochemical recognition, liquid crystalinity, charge transport, catalysis, or nanoparticles [3–6]. It has found application as an electron-active building block for elaborating switching molecular aggregates [7], redox-active receptors [8], and conducting and magnetic materials [9]. Ferrocene has a low-lying triplet excited state and it is known to be an effective triplet quencher [10]. Due to the structural and electrochemical properties it is also known to be a good electron donor [11, 12], ferrocene-containing tetrathiafulvalene (*TTF*) derivatives have been constructed as donors for conducting charge transporting (CT) complexes. The first compound belongs to this class of heterocyclic donor conducting materials [13] and very similar types of donor heterocycles have been reported also in literature [14]. On the other hand, typical non-linear optical (NLO) chromophores for applications in optoelectronics and photonics are conjugated π-systems of the A-bridge-D type with strong acceptor (A) and donor (D: ferrocene) groups as terminal substituents [15]. Over the last several years polymers containing ferrocene moieties have been prepared, and many studies on ferrocene containing dimers and oligomers have been reviewed [16, 17].

It also has to be noted that a variety of transporting materials (TM), involving hydrazone, stilbene, pyrazoline, arylalkane, arylamine, oxadiazole, or

* Corresponding author. E-mail: vgetaut@ktu.lt

benztriazole moieties have been generated in recent years [18]. Rapid charge transporting ability, high photosensitivity, simple synthesis, and low price are the advantages of the hydrazones against others hole transporting materials. Unfortunately, low molecular weight TM containing hydrazone moieties are usually crystalline materials, are not capable of forming thin neat homogenous layers, and must be used in combination with polymeric hosts. Therefore it is of interest and significance to develop photo- and electroactive low-molecular-weight amorphous materials and polymers that form stable amorphous glasses having glass-transition temperatures above room temperature. These compounds could form stable films with less or even without binder materials, and are expected to manifest properties and functions more

effectively relative to molecularly doped polymer compositions.

These findings prompted us to synthesize and characterize new charge transporting materials (CTM) incorporating the ferrocene and hydrazone moieties and to study the morphological, optical, and photoconductive properties of these compounds. We also preliminary investigate these molecular glasses and polymer as CTM for electrophotography.

Results and Discussion

The synthesis of new ferrocene containing molecular glasses and polymer was carried out by a multi-step reaction. The first step was a condensation of ferrocenecarboxaldehyde with bis(4-hydrazinophenyl)sul-
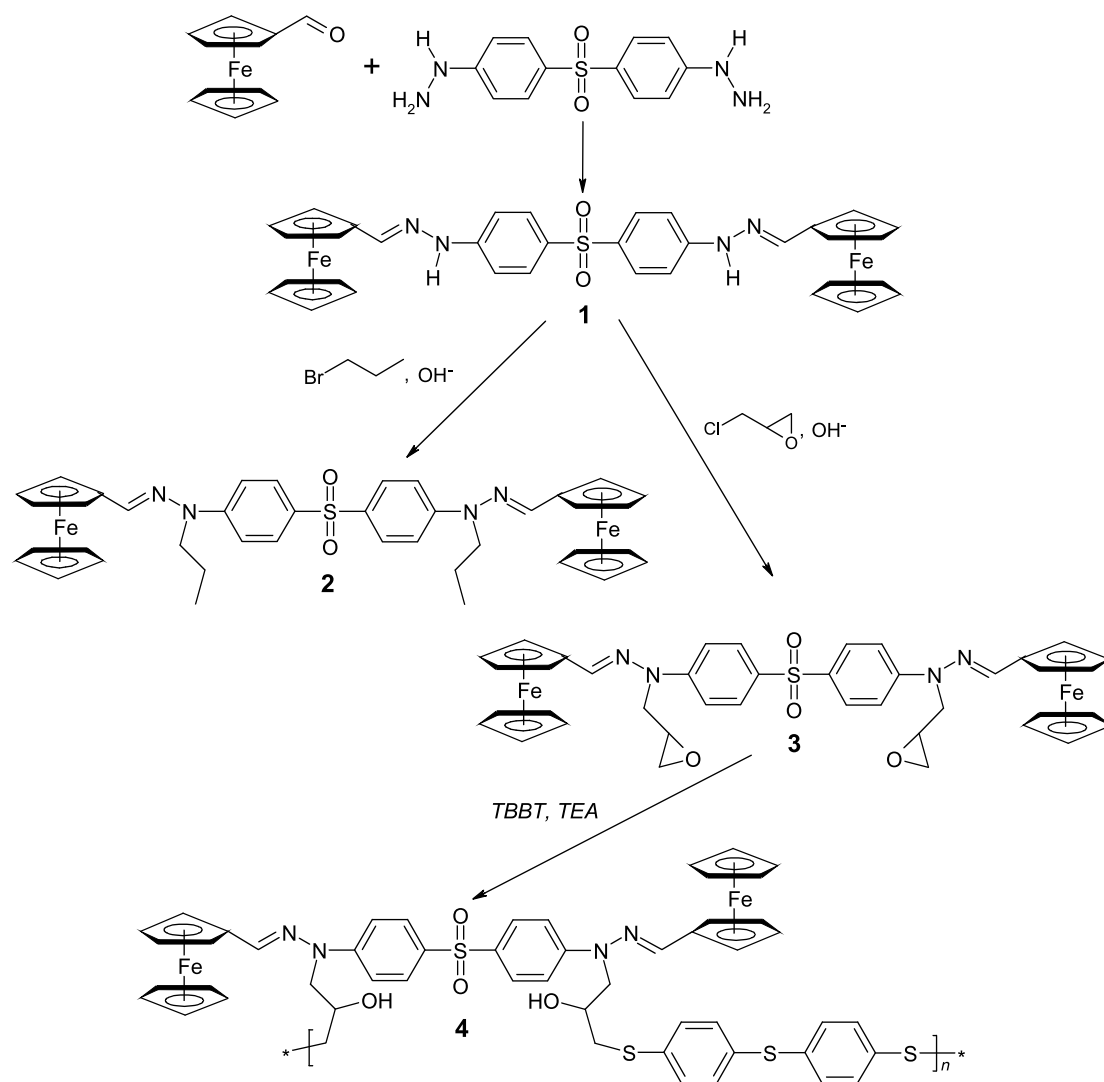
Scheme 1

fone to obtain the intermediate compound bis{4,4′-[2-(ferrocen-2-ylmethylen)hydrazin-1-yl]phenyl}-sulfone (**1**). By interaction of this dihydrazone with epichlorohydrin in the presence of KOH, bis{4,4′-[2-(ferrocen-2-ylmethylen)-1-(2,3-epoxypropyl)hydrazin-1-yl]phenyl}sulfone (**3**) was prepared (Scheme 1). Moreover, a model compound bis{4,4′-[2-(ferrocen-2-ylmethylen)-1-propylhydrazin-1-yl]phenyl}sulfone (**2**) was synthesized by alkylation of **1** with 1-brompropane in the presence of potassium hydroxide.

Finally, the polyaddition of the monomer **3** with 4,4′-thiobisbenzenethiol in *THF* was carried out in the presence of the catalyst triethylamine (*TEA*) at the reflux temperature of *THF*. The polymer **4** possessing both ferrocene and hydrazone moieties was isolated in 86% yield. The average molecular weights and their distribution were detected by gel permeation chromatography (GPC) and are presented in Table 1.

Formation of the glassy state of **2**–**4** was confirmed by differential scanning calorimetry (DSC) analysis. The melting points (T_m) and glass transition temperatures (T_g) of the TM are presented in

Table 1. Characteristics of compounds **2**–**4**

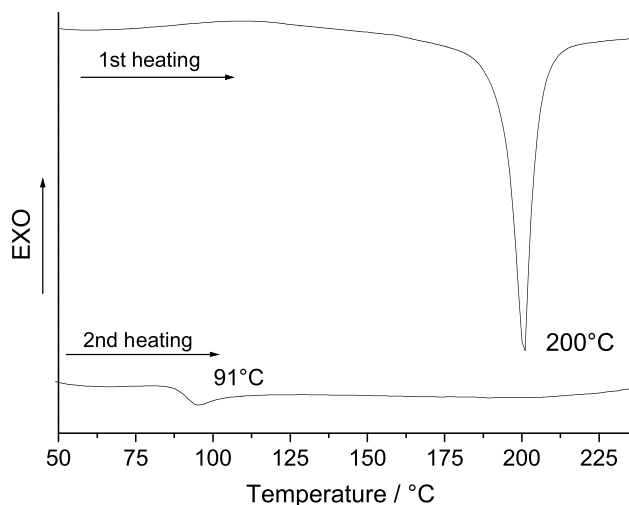| Compound	$\overline{M_N}/$ gmol^{-1}	$\overline{M_W}/$ gmol^{-1}	$\dfrac{\overline{M_W}}{\overline{M_N}}$	$T_g/°C$	I_p/eV
2	–	–	–	91	5.35
3	–	–	–	108	5.40
4	2200	13400	6.09	148	5.41

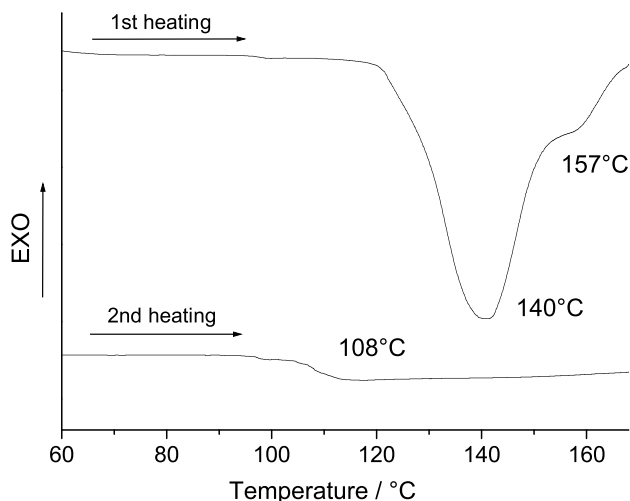**Fig. 1.** DSC first and second heating curves of **2** (heating rate 10 K/min)

Fig. 2. DSC first and second heating curves of **3** (heating rate 10 K/min)

Table 1. These investigations revealed that the model compound **2** and the monomer **3** can exist both in the crystalline and amorphous state. In Fig. 1 there are presented DSC first and second heating curves for **2**. The DSC curve for **2** at first heating reveals a melting at 200°C, no crystallization takes place during cooling or second heating, only a glass transition at 91°C is registered during the second heating. The material remains in the glassy state after melting and subsequent cooling; this is a common feature for both dihydrazones investigated here. A similar picture was observed for the diepoxyde **3** (Fig. 2). The sample produced endotherminc polymorphic melting transitions at 140°C and 157°C during the first heating cycle, did not subsequently crystallize when cooled, and exhibited a glass transition temperature of 108°C during the second heating. Therefore, **2** and **3** can be considered as molecular glasses. Formation of the glassy state in the ferrocene containing polymer **4** (Fig. 3) was observed at 148°C.

A change of the alkyl fragment from propyl to epoxypropyl, leads to an increase of T_g by ca. 17°. The T_g temperature rises by another 40° if we compare monomer **3** with polymer **4**. Thus, the DSC data demonstrated that the T_g increased as the molecular size and weight of the compounds increases.

Since π-electrons are very important for the charge transporting process in the TM structures, the UV-Vis absorption spectra of the ferrocene containing dihydrazones **2**, **3**, and polymer **4** are given in Fig. 4. The spectra of ferrocenecarboxaldehyde (*Fc*) and 4,4′-thiobisbenzenethiol (*TBBT*) are given for com-
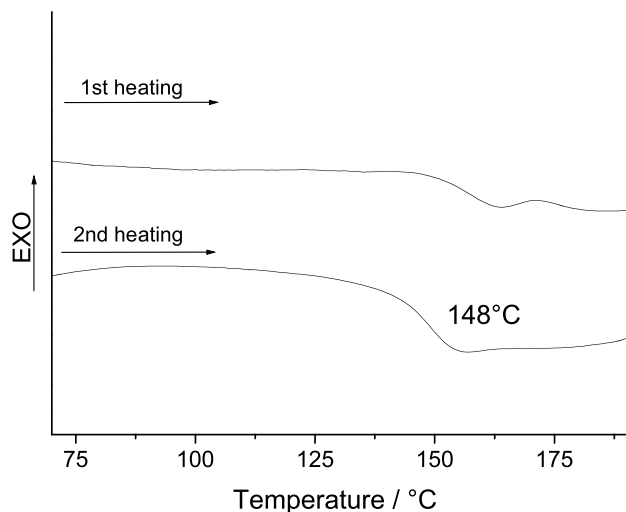
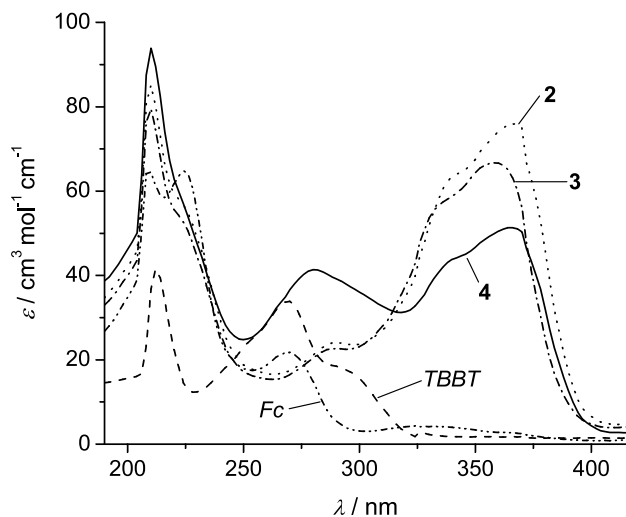**Fig. 3.** DSC first and second heating curves of **4** (heating rate 10 K/min)

Fig. 4. UV-Vis absorption spectra (*THF*, $c = 10^{-4}$ *M*) of **2–4**, *Fc*, and *TBBT*

Fig. 5. Photoemission (in air) spectra of the TM

parison. The absorption spectra of dihydrazones **2**, **3**, and polymer **4** exhibit a very strong hyperchromic and bathochromic ($\approx$90 nm) shift, attributed to $\pi \rightarrow \pi^*$ transitions with respect to the spectrum of ferrocenecarboxaldehyde. This is the consequence of the greatly increased conjugated π-electron system of the ferrocene containing hydrazones in comparison with the bare ferrocenyl chromophore. Moreover, this shift is also attributed to the presence of conjugated donor and acceptor groups in these molecules. On the other hand, introduction of the epoxypropyl groups in **3** instead of propyl has a minor hypsochro-
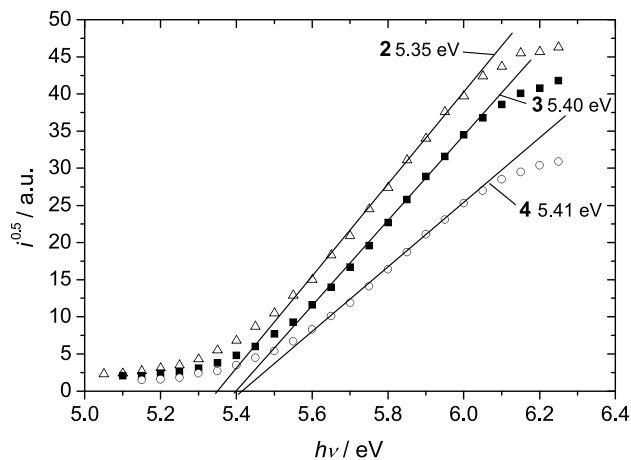
mic effect ($\approx$6 nm) compared with **2**. Difference in π-electron conjugation between the corresponding monomer **3** and polymer **4** is not very significant ($\approx$6 nm), which proves that conjugated π-electron systems remain intact during the polyaddition reaction. Moreover, the introduction of the linking fragment *TBBT* into the molecule of the polymer **4** can be clearly observed in the 280 nm region of UV spectrum due to the $\pi \rightarrow \pi^*$ transitions of this fragment.

Figure 5 shows the electron photoemission spectra of the films of ferrocene containing dihydrazones **2**, **3**, and **4**. The ionization potential (I_p) values established from these spectra correlate with the UV absorption data. The I_p for dihydrazone **2** is 5.35 eV, replacement of the propyl group by the epoxypropyl leads to the increase of I_p to 5.40 eV for **3**, I_p for polymeric TM **4** is 5.41 eV. The I_p values of these compounds show that they are suitable for the application in electrographic photoreceptors, as it is widely known that holes are easily injected into the charge transport layer from the charge generation layer with I_p close to I_p of charge transport layer. The I_p values for charge transporting materials, including those widely used with pigments in electrophotographic photoreceptors, such as titanyl phthalocyanines, are in the range of 5.1–5.6 eV [19].

The compounds **2–4** are soluble in common organic solvents, such as chloroform, *THF*, dioxane, *etc*. This really good solubility is mainly attributed to the flexible aliphatic chains or linking fragments between chromophores (in case of polymer). Clear, transparent, and homogeneous films of **2–4** doped into polycarbonate (*PC-Z*) were obtained by the casting technique.

Table 2. Mobility data

Layer composition	$\mu_0/$ $cm^2 V^{-1} \cdot s^{-1}$	$\mu/$ $cm^2 V^{-1} \cdot s^{-1,*}$	$\alpha/$ $(cm/V)^{0.5}$
2 + *PC-Z*	2×10^{-10}	2.8×10^{-8}	0.006
3 + *PC-Z*	1.5×10^{-10}	1.4×10^{-8}	0.0057
4 + *PC-Z*	7.5×10^{-10}	7.8×10^{-8}	0.0058

* At an electric field 6.4×10^5 V cm^{-1}

The preliminary hole drift mobility was measured by the xerographic time of flight technique and results are presented in Table 2. The hole drift mobility values in compositions of dihydrazones **2**, **3**, and **4** with *PC-Z* exceeded 10^{-8} cm^2/Vs at an electric field of 6.4×10^5 V/cm. More detailed investigations of applications and photoelectric properties of this novel family of CTM will be described in publications to follow.

In conclusion, novel ferrocene and dihydrazone containing hole transporting monomer and polymer were synthesized and their optical, morphological, and photoconductive properties were investigated. This study showed that the designed new structures possessing both ferrocene and hydrazone moieties may be candidates for hole transporting materials of organic photoreceptors.

Experimental

The ^{1}H NMR spectra were taken on Varian Unity Inova (300 MHz) spectrometer at room temperature. The course of the reactions products were monitored by TLC on Silufol UV-254 plates (eluent: acetone:*n*-hexane = 7:18) and development with I$_2$ or UV light. Silica gel (grade 62, 60–200 mesh, 150 Å, Aldrich) was used for column chromatography. Elemental analyses were performed with an Exeter Analytical CE-440 Elemental; their results agreed satisfactorily with the calculated values. The UV spectra were recorded on a Spectronic Genesys 8 spectrometer in *THF*. 10^{-4} *M* solution of investigated TM and microcell with an internal width of 2 mm was used. IR-spectroscopy was performed on a Perkin Elmer Spectrum BX II FT-IR System, using KBr pellets. Thermal transition data for synthesized compounds possessing hydrazone moieties was collected using a TA Instruments Q100 and Mettler DCS 30 Differential Scanning Calorimeters An empty Al pan was used as the reference. Samples of 5–8 mg as obtained from the synthesis were heated in Al pans at a scan rate 10 K/min under a N$_2$ flow. During the first heating the melting points were measured. After melting, the samples were cooled with the same rate. The resulting glasses were heated again under the same conditions to measure the glass transition temperatures (T_g). The average molecular weight and the molecular weight distribution were estimated by gel permeation chromatography using a GPC system including a

Bischoff Lambda 1000 UV detector (256 nm), Spectra-Physics SP8800 pump, Viscotek DM 400 data collecting unit and Viscotek GMH$_{HR}$-M and G2500H$_{HR}$ columns using *THF* as eluant. Polystyrene standards were used for column system calibration. The collected data was processed using Omni SEC version 3.0.1 software. The samples for the ionisation potential measurement were prepared by dissolving materials in *THF* and were coated on Al plates pre-coated with ∼0.5 μm thick methylmethacrylate and methacrylic acid copolymer adhesive layer. The thickness of the transporting material layer was 0.5–1 μm. The ionization potential (I_p) was measured by the photo-emission in air method, similar to the one used in Ref. [20]. Usually the photoemission experiments are carried out in the vacuum and high vacuum is one of the main requirements for these measurements. If vacuum is not high enough the sample surface oxidation and gas adsorption are influencing the measurement results. In our case, however, the organic materials investigated are stable enough to O$_2$ and the measurements may be carried out in the air. The samples were illuminated with monochromatic light from the quartz monochromator with a D lamp. The power of the incident light beam was $(2–5) \times 10^{-8}$ W. A negative voltage of -300 V was supplied to the sample substrate. The counter-electrode with the 4.5×15 mm^2 slit for illumination was placed at 8 mm distance from the sample surface. The counter-electrode was connected to the input of the BK2-16 type electrometer, working in the open input regime, for the photocurrent measurement. The 10^{-15}–10^{-12} A strong photocurrent was flowing in the circuit under illumination. The photocurrent I is strongly dependent on the incident light photon energy $h\nu$. The $I^{0.5} = f(h\nu)$ dependence was plotted. Usually the dependence of the photocurrent on incident light quanta energy is well described by a linear relationship between $I^{0.5}$ and $h\nu$ near the threshold [20, 21]. The linear part of this dependence was extrapolated to the $h\nu$ axis and I_p value was determined as the photon energy at the interception point. The samples for mobility measurements were prepared from solutions in *THF* of pure TM and 1:1 mass proportion compositions of TM with Polycarbonate-Z (Iupilon Z-200 from Mitsubishi Gas Chemical Co.). The layer thickness was in the range 5–10 μm. The sample substrate consisted of polyester film with a conductive Al layer. The hole drift mobility was measured by the xerographic time of flight (*XTOF*) technique [22–24]. Positive corona charging created an electric field inside the TM layer. Charge carriers were generated at the layer surface by illumination with pulses of a N$_2$ laser (pulse duration was 2 ns, wavelength 337 nm). The intensity of pulse was small and layer surface potential decrease did not exceed 1–5% of the initial potential. Therefore it can be assumed that electric field is not changed and charge carriers drift in the initial electric field. The rate of the surface potential decay dU/dt was measured using an electrometer having a capacitance probe and operating in the differentiation mode. The charge carrier transit time t_t was determined by the kink on the dependence of the dU/dt on time. This dependence was presented in the linear scale or for the more precise determination of t_t double logarithmic scale. The drift mobility was calculated using $\mu = d^2/U_0 t_t$, where d is the layer thickness and U_0 is the surface potential at the moment of illumination.

Bis{4,4′-[2-(ferrocen-2-ylmethylen)-hydrazin-1-yl]phenyl} sulfone (**1**, $C_{34}H_{30}Fe_2N_4SO_2$)

A mixture of 10 g ferrocenecarboxaldehyde (0.0467 mol) and 6.18 g bis(4-hydrazinophenyl)sulfone (0.0222 mol, prepared as described in Ref. [25]) was dissolved in 110 cm³ dioxane. After stirring at 60°C for 2 h, the reaction mixture was cooled to room temperature. The crystals formed upon cooling were filtered and washed with 2-propanol to yield 10.7 g (71.9%) of the dihydrazone intermediate, which was used as it was in the next step. ¹H NMR (300 MHz, DMSO-d₆): $\delta = 10.56$ (s, NH), 7.76 (s, CH=N), 7.66 (d, $J = 9$ Hz, 4H, 2-H, 6-H Ar), 7.03 (d, $J = 9$ Hz, 4H, 3-H, 5-H Ar), 4.60 (m, 4H, of subst. cyclopentadiene), 4.35 (s, 4H, of subst. cyclopentadiene), 4.16 (s, 10H, unsubst. cyclopentadiene) ppm; IR (KBr): $\bar{\nu} = 3257$ (NH), 3099, 3033, 3000 (CH aromatic), 2954, 2886, 2854 (CH aliphatic), 1593 (C=C), 1102 (SO₂) cm⁻¹.

Bis{4,4′-[2-(ferrocen-2-ylmethylen)-1-propylhydrazin-1-yl] phenyl}sulfone (**2**, $C_{40}H_{41}Fe_2N_4SO_2$)

To a 100 cm³ 3-neck round bottom flask equipped with reflux condenser, 2.50 g **1** (3.73 mmol) and 20 cm³ 1-brompropane (0.21 mol) were added. The reaction mixture was refluxed for 4 h, during which 0.74 g powdered 85% KOH (11.19 mmol) and 0.24 g anh. Na₂SO₄ (3.73 mmol) were added in three portions. The mixture was cooled to room temperature and filtered off. The organic part was treated with ethyl acetate and washed with distilled H₂O until neutral. The organic layer was dried (MgSO₄), treated with activated charcoal, filtered and, the solvents were removed. The residue was purified by column chromatography using silica gel (grade 62, 60–200 mesh, 150 Å, Aldrich) and an eluent mixture (acetone:*n*-hexane 3:22, v/v). The solid was recrystallized from this mixture and dried at 50°C in a vacuum oven. The yield of **2** was 1.86 g (66%), mp 202–204°C. ¹H NMR (300 MHz, DMSO-d₆): $\delta = 7.81$ (d, $J = 8.7$ Hz, 4H, 2-H, 6-H Ar), 7.45 (s, CH=N), 7.29 (d, $J = 8.7$ Hz, 4H, 3-H, 5-H Ar), 4.61 (s, 4H, 2-H, 5-H of subst. cyclopentadiene), 4.33 (s, 4H, 3-H, 4-H of subst. cyclopentadiene), 4.14 (s, 10H, unsubst. cyclopentadiene), 3.78 (t, $J = 7.2$ NCH₂), 1.76–1.56 (m, 4H, C$\underline{H_2}$CH₃), 1.03 (t, $J = 7.5$ Hz, CH₃) ppm.

Bis{4,4′-[2-(ferrocen-2-ylmethylen)-1-(2,3-epoxypropyl) hydrazin-1-yl]phenyl}sulfone (**3**, $C_{40}H_{38}Fe_2N_4SO_4$)

To a 100 cm³ 3-neck round bottom flask equipped with reflux condenser, thermometer dihydrazone intermediate **1** 3.94 g (5.88 mmol) and 10.3 cm³ epichlorohydrin (0.13 mol) were added. The reaction mixture was stirred vigorously at 35–40°C for 3 h, during which 1.72 g powdered 85% KOH (0.026 mol) and 0.5 g anh. Na₂SO₄ (0.0035 mol) were added in three portions with prior cooling of the reaction mixture to 20–25°C. Then the mixture was cooled to room temperature and filtered. The organic part was treated with ethyl acetate and washed with distilled H₂O until neutral. The organic layer was dried (MgSO₄), treated with activated charcoal, filtered, and solvents were removed. The residue was purified by column chromatography using silica gel (grade 62, 60–200 mesh, 150 Å, Aldrich) and an eluent mixture (acetone:*n*-hexane 3:22,

v/v). The solid was recrystallized from this mixture and dried at 50°C in a vacuum oven. The yield of **3** was 2.08 g (45%), mp 145–147°C. ¹H NMR (300 MHz, DMSO-d₆): $\delta = 7.81$ (d, $J = 9.1$ Hz, 4H, 2-H, 6-H Ar), 7.63 (s, CH=N), 7.34 (d, $J = 9.1$ Hz, 4H, 3-H, 5-H Ar), 4.64–4.60 (m, 4H, 2-H, 5-H of subst. cyclopentadiene), 4.40–4.32 (m, 6H, 3-H, 4-H of subst. cyclopentadiene, one of NCH₂ protons), 4.15 (s, 10H, unsubst. cyclopentadiene), 3.93–3.83 (dd, (H_A), $J_{AX} = 4.5$ Hz, $J_{AB} = 16.6$ Hz, another of NCH₂ protons), 3.30–3.20 (m, CHO), 2.84 (dd, (H_A), $J_{AX} = 4.2$ Hz, $J_{AB} = 4.8$ Hz, one of CH₂O protons), 2.57 (dd, (H_B), $J_{BX} = 2.7$ Hz, another of CH₂O protons) ppm; IR (KBr): $\bar{\nu} = 3084$ (CH aromatic), 2995, 2954, 2925, 2854 (CH aliphatic), 1588, 1498 (C=C, C–N), 1102 (SO₂) cm⁻¹.

Poly[bis{4,4′-[2-(ferrocen-2-ylmethylen)-1-(2,3-epoxypropyl)hydrazin-1-yl]phenyl}sulfone-alt-4,4′-tiobisbenzenethiol] (**4**, $(C_{52}H_{48}Fe_2N_4S_4O_4)_n$)

0.75 g compound **3** (0.96 mmol), 0.24 g 4,4′-thiobisbenzenethiol (0.96 mmol) and 0.13 cm³ TEA (0.96 mmol) were refluxed in 15 cm³ THF under Ar for 60 h. The reaction mixture was cooled to room temperature and filtered through a 3–4 cm layer of silica gel (grade 62, 60–200 mesh, 150 Å) and the silica gel was washed with THF. The solution was concentrated to 15–20 cm³ by evaporation and then poured into a 20-fold excess of methanol with intensive stirring. The resulting precipitate was filtered off and dried under vacuum at 50°C. The yield of **4** was 0.85 g (86%). ¹H NMR (300 MHz, DMSO-d₆): $\delta = 7.88$–7.55 (m, 6H, CH=N, 2-H, 6-H Ar), 7.50–7.08 (m, 12H, Ar), 5.58 (s, OH), 4.54 (s, 4H, 2-H, 5-H of subst. cyclopentadiene), 4.30 (s, 4H, 3-H, 4-H of subst. cyclopentadiene), 4.21–3.87 (m, 14H, unsubst. cyclopentadiene, NCH₂), 3.61–3.44 (m, CH); 3.30–3.01 (m, CH₂) ppm; IR (KBr): $\bar{\nu} = 3473$ (OH, broad), 3091 (CH aromatic), 2915 (CH aliphatic), 1587, 1497, 1475 (C=C, C–N, C=N), 1102 (SO₂), 818 (CH=CH of 1,4-disubstituted benzenes) cm⁻¹.

Acknowledgements

References

[1] Hudson RDA (2001) J Organomet Chem **637**: 47

[2] Balavoine GGA, Daran JC, Iftime G, Lacrolx PG, Manoury E, Delaire JA, Maltey-Fanton I, Natatani K, Bella SD (1999) Organometallics **18**: 21

[3] Zhu Y, Clot O, Wolf MO, Yap GPA (1998) J Am Chem Soc **120**: 1812

[4] Templeton AC, Wuelfing WP, Murray RW (2000) Acc Chem Res **33**: 27

[5] Tongi A, Hayashi T (1995) In: Tongi A, Hayashi T (eds) Ferrocenes, Homogeneous Catalysis, Organic

Synthesis and Materials Science, VCH, Weinheim, p 271

[6] Manners I (1995) Adv Organomet Chem **37**: 131

[7] Medina JC, Gay I, Chen Z, Echegoyen Z, Gokel GW (1991) J Am Chem Soc **113**: 365

[8] Houlton A, Jasim N, Roberts RMG, Silver J, Ham DC, Mcardle P, Higgins T (1992) J Chem Soc Dalton Trans 2235

[9] Green MLH, Qin J, Hare DO (1998) J Organomet Chem **358**: 375

[10] Bhattacharyya K, Ramaiah D, Das PK, Geoge MV (1996) J Phys Chem **90**: 5984

[11] Watts WE (1979) J Organomet Chem Libr **7**: 300

[12] Imahori H, Norieda H, Yamada H, Nishimura Y, Yamazaki I, Sakata Y, Fukuzumi S (2001) J Am Chem Soc **123**: 100

[13] Ueno Y, Sano H, Okawara M (1980) J Chem Commun 28

[14] Moore AJ, Skabara PJ, Bryce MR, Batsanov AS, Howard JAK, Daley STAK (1993) J Chem Soc Chem Commun 417

[15] Perepichka IF, Perepichka DF, Bryce MR, Chesney A, Popov AF, Khodorkovsky V, Meshulam G, Kotler Z (1999) Synth Met **102**: 1558

[16] Zhu Y, Wolf MO (1999) Chem Mater **11**: 2995

[17] Barlow S, O'Hare D (1997) Chem Rev **97**: 637

[18] Borsenberger PM, Weiss DS (1993) In: Borsenberger PM, Weiss DS (eds) Organic Photoreceptors for Imaging Systems, Marcel Dekker, New York, p 447

[19] Borsenberger PM, Weiss DS (1993) In: Borsenberger PM, Weiss DS (eds) Organic Photoreceptors for Imaging Systems, Marcel Dekker, New York, p 273

[20] Miyamoto E, Yamaguchi Y, Yokoyama M (1989) Electrophotography **28**: 364

[21] Cordona M, Ley L (1978) Top Appl Phys **26**: 1

[22] Montrimas E, Gaidelis V, Pazera A (1966) Lith J Phys **6**: 569

[23] Vaezi-Nejad SM (1987) Int J Electron **62**: 361

[24] Archie Y, Chan C, Juhasz C (1987) Int J Electron **62**: 625

[25] Connell JW, Bass RG, Sinsky MS, Waldbauer RO (1987) J Polym Sci, A: Polym Chem **25**: 2531